Energy 118 (2017) 197–208

Contents lists available at ScienceDirect

Energy

journal homepage: www.elsevier.com/locate/energy

A flexible control strategy of plug-in electric vehicles operating in seven modes for smoothing load power curves in smart grid

Siwar Khemakhem, Mouna Rekik, Lotfi Krichen*

National Engineering School of Sfax, Control and Energy Management Laboratory (CEMLab), BP 1173, 5052, Sfax, Tunisia

ARTICLE INFO

Article history:
Received 15 August 2016
Received in revised form
30 November 2016
Accepted 11 December 2016

Keywords:
Plug-in electric vehicles
Lithium-ion battery
Smart grid
Supervision strategy
Load power variance

ABSTRACT

Plug-in electric vehicles (PEVs) seem to be an interesting new electrical load for improving the reliability of smart grid. The purpose of this work is to investigate a supervision strategy based on regulated charging of PEVs in order to guarantee an optimized power management of the system and consequently a flatter power demand curve. The system mainly includes PEVs powered by a Lithium-ion battery ensuring the charging and discharging operations of these PEVs at home and a daily load power demanded by home appliances. The purpose of the considered strategy is to detect the connection status of each PEV and to establish the priority order between these PEVs with certain flexibility which results in managing the PEVs through seven operating modes. The response of the control algorithm enables to ensure the power flow exchange between the PEVs and the electrical grid, especially at rush hours, and to minimize load power variance aiming to achieve the smoothness for the power demand curve and to reduce the stress of the electrical grid. The simulation results are presented in order to illustrate the efficiency of this power control approach.

1. Introduction

Up-to-date, the world has undergone a challenge in terms of providing electricity and ensuring global energy requirements. The challenge is mainly due to the shortage of primary energy resources from conventional fossil fuels like natural gas, coal and oil [1]. As a result, there is a great tendency to integrate the renewable energy resources and the use of plug-in electric vehicles (PEVs) on the smart grid in order to minimize reliance on conventional energy resources, satisfy the energy demands and consequently decreasing concerns related to global warming effects as well as the ones related to energy crisis [2–5].

The excessive electricity consumption causes intense surges in demand during peak hour which can cause undesirable impacts and harm the stability of the existing network. That's why; some researchers are working on ways to minimize load power variance by using renewable energy sources. In Ref. [6], a stochastic multi-objective daily volt/var control based on hydro-turbine, fuel cell, wind turbine, and photovoltaic power plants are investigated. A study in Ref. [7] has developed a new control strategy that involves wind and photovoltaic generation subsystems. This strategy has been suggested with the objective of load power demand satisfaction, storage and grid constraints verification in order to avoid blackout. These methods have presented good solutions to reduce load power variance and enhance power electrical system quality. However, the common disadvantage of this renewable distributed generation is their intermittent and unstable production due to their dependence on weather change and climatic fluctuation. Currently, power systems supervision has been changing leading to accomplish renewable energies gaps and use new paradigms in the functioning and improvement of power systems.

Plug-in Electric Vehicles (PEVs) as an emerging new electrical load and a significant approach on smart grid, have attracted more attention worldwide and have appeared as future solution towards solving problems for the energy management owing to their mobility and power storage properties [8,9].

In that, smart grid as a suitable concept has a potential to improve grid modernization for making it more able to address future need, more efficient and accommodating [10]. Some researchers are interesting in smart meters, electricity storage technologies, and electrical local smart grids in which they develop the design of coherent smart energy systems as an integrated part of achieving future 100% renewable energy and transport solutions [11,12]. Ref. [13] has presented the interest profits, risks and a

* Corresponding author.
E-mail address: lotfi.krichen@enis.rnu.tn (L. Krichen).

http://dx.doi.org/10.1016/j.energy.2016.12.039

challenge concerned in smart grid and has insisted on the impact of the actual smart grid modernization for potential and reliable energy generation. Indeed, the need for new flexible electric power with quality improvement leads to the development of the bidirectional flow of electricity and information [14]. Communications flow is used to collect data supplied by meters and sensors that can be used to permit both consumers and utilities to reply to the grid status [15]. In this context, these PEVs are equipped by batteries which can operate as a load on the grid known as grid-to-vehicle (G2V) concept or as a power source known as vehicle-to-grid (V2G) concept [16,17]. It has been proved that the V2G technology can describe an interactive relationship between PEVs and the power grid [18,19], help to realize the balance between production and consumption of power grid, participate in frequency regulation [20], so as to flatten the variation of the load power profiles [21], reduce cost [22] and integrate renewable energy sources [23]. From these interesting benefits, various researches have been carried out the PEVs and their integration into the grid. Ref. [24] discusses the impact of PEVs and V2G technology to integrate a highly level of wind generation without excess on electricity production as well as greatly to minimize national CO2 emissions. Ref. [25] describes the main challenge of renewable energy strategies to include the transportation field in these strategies for sustainable development purpose and discusses the potential solutions for this challenge in Denmark case. Authors in Ref. [26] have concentrated on the notions of G2V concept and V2G technology, their economic benefits depending on the charging strategies of PEVs (coordinated/uncoordinated charging) and their effects on power distribution networks. Others in Ref. [27] are working on the optimal scheduling of charging/discharging behavior of electrics vehicles. They are adjusting the PEVs power and are proposing a locally optimal scheduling scheme.

Researchers in Ref. [28] are working on the performance of batteries for PEVs. They have exanimate the recent battery technologies for PEV and the most important parameters to maximize the effectiveness and competitiveness of PEV battery on short and long term. Ref. [29] has presented an estimated sample model-based health management of Lithium-ion batteries for electrified vehicles to maintain the battery lifecycle. A study in Ref. [30] has explained new dynamic model at battery swapping station for electric vehicles in electricity market.

Within the smart grid concept, much studies has been concentrated on the active participation of demand-side response, household electricity use and smart homes in terms of their structures, components, and benefits [31–33]. An overview of services offered by smart home and reveals key barriers to smart home adoption was carried out in Ref. [34]. Authors in Ref. [35] focus on the prediction of the next day energy consumption for smart homes. Others in Ref. [36] proposed a home energy management system to manage household energy consumption aiming to keep the customer comfort at a good condition. Moreover, there are several studies aiming to reduce load power variance. For instance, an energy retailer scheme that permits investigating demand response in electricity supply is presented in Ref. [37] in order to achieve load minimizing based on price elasticity using Power Systems Computer Aided Design (PSCAD). An improvement of the load variance in household smart micro-grid using charging profiles of plug-in hybrid electric vehicles driven by the residents was explored in Ref. [38].

Although these considered studies have elaborated different aspects for PEVs charge scheduling, energy loss minimization and consequently load power variance enhancing, however, it is notable that there is not enough flexibility either in PEV time connection, or in energy demand as well in duration of charging.

In this paper, a flexible control strategy of PEV operating in seven modes is proposed. The aim is to satisfy the energy dispatching between PEVs and power grid and to minimize the load power variance. For that, an appropriate algorithm must be achieved to generate the optimal required powers and avoid the high electricity demand in peak hours. In fact, the main contribution of this work is to monitor the system under different operation modes of activation according to the following constraints: (i) the daily load demand of the household appliances, (ii) the connection time of the each PEV, (iii) the priority order and the state of charge (SOC) value of each battery.

The algorithm presented is flexible and applicable for any house equipped with two PEVs which could provide grid support by injection or absorption of their optimal reference powers when charging slot time that are available at home.

The flexibility of this approach is shown in PEV time connection and their charge/discharge duration. Indeed, the bidirectional energy flow of vehicle to home (V2H) provides greater flexibility to control the PEV battery energy which is one of the recent technologies. It can be considered not only as an electric load but also as a storage system and thus a supplier of electrical demand at home appliances. The focus of this considered strategy is thus, firstly, the detection of the presence of each PEV taking into account the priority selection of PEV owner chosen charging time period, and secondly, the availability of these PEVs to switch between many power flow feasibilities according to seven operating modes with a flexibility degree in order to achieve a flatter daily power demand curve.

The paper is structured as follows: section 2 shows the description of the studied system and the modeling of the battery as an important electrical part in exchanging power for each PEV. Section 3 details the control of PEV power generation. In section 4, the power control algorithm applied to the studied PEVs taking into account their connection status to the grid will be described. A flexible strategy is investigated to show the impact of this regulated charging on minimizing load power variance and flattening consequently the daily power demand curve. The simulation results and the conclusion of this work are developed in sections 5 and 6, respectively.

2. System description and modeling

2.1. System description

The aim of this paper is to point out the high power of PEVs which could provide significant flexibility in their connection time and duration of charging when they are parked at home and to demonstrate the appropriate merits of V2G technology. As shown in Fig. 1, the studied home is equipped by AC powered devices, DC powered devices associated to DC/AC power converters to connect these load to the AC power grid and PEVs with their bidirectional chargers.

Each PEV includes a Li-ion battery pack, an inductive filter L, a bidirectional DC/DC converter, a DC link voltage bus, a bidirectional DC/AC converter and a line which is represented as an RL filter.

The direction of the current is the criterion to define the charge or discharge phase of the battery. Positive battery current determines the discharging operation and negative battery current determine the charging process. The L filter participates into the chopper operation and smoothes the charge and discharge current ripples. This inductor filter and the buck-boost DC/DC converter are used to ensure the possibility of bidirectional power flow exchange (charge/discharge) and to adjust the voltage levels between the battery pack and the DC bus. Therefore, the DC/DC converter aims to adapt the battery output voltage to the appropriate inverter input voltage. The bidirectional DC/AC converter which is

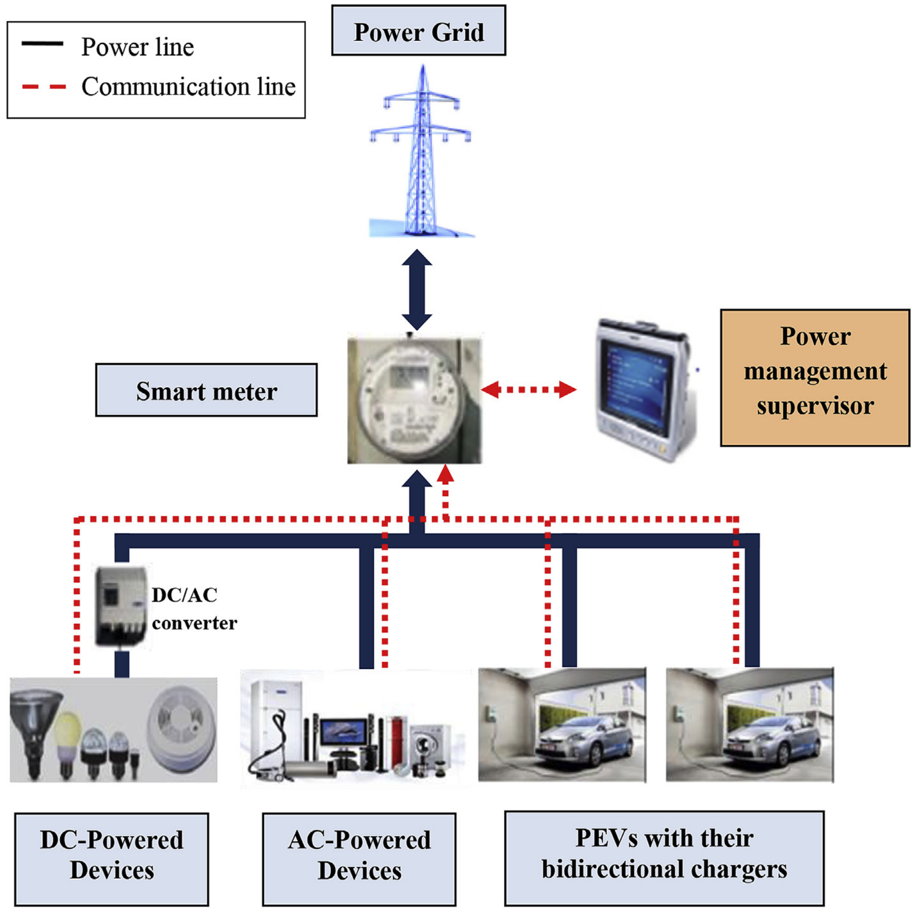

Fig. 1. Scheme of home components.

interposed between the DC bus and the line achieves the energy transit from the DC bus to the appropriate AC values in order to inject (or absorb) sinusoidal currents into the electrical grid [39]. This converter acts as a rectifier in charging mode and as an inverter in discharging mode. The RL filter is used to improve the quality of current injected or absorbed to the grid, to attenuate harmonics caused by the DC/AC converter and guarantee a three-phase voltage source to attain a quasi sinusoidal voltage. The integration of both communication and electrical power flows is the essential characteristic of smart grid. The modern technologies in the smart metering are essential to ensure a successful integration of PEVs framework V2G concept, a dynamic PEV load as well as effective information measured of the power demanded or supplied to grid [40]. For that, it is assumed in this paper that each PEV have two flows when it is plugged-in. In addition, a "flexible supervision strategy of PEVs powers" is proposed to switch between different operating modes, to ensure the dispatch of power between PEVs and smart grid in a flexible way depending on the information obtained by the smart meter, so as to reduce the load power variance and highly achieve the efficiency of the load power curve. This strategy is applicable in any home in which the base load of the household appliances is defined from the typical daily load profile.

2.2. Modeling of the battery

The PEV modeling will gain importance in the electric part. The battery has an important effect on the V2G systems. This electrical component assumes the power exchange between the PEV and the power grid. The battery model in this study, as it is considered as the most recent battery technology used in PEVs, is based on a commercially lithium-ion (Li-ion). Lithium-ion battery was selected in this work because the cell battery has a significant energy densities, high specific power, long lifetime, lightweight nature, security, lower cost, lower waste of charge, and, potentially higher voltage [41–43]. The simplest form of the "electrical battery model" is a voltage source connected in series with an internal resistance. It can be distinguished that there is a characteristic equation of the battery voltage, for each operating mode.

The voltage source is modeled by the charge equation of lithium-ion battery as follows [44]:

$$V_{batt} = U_0 - R \cdot i - K \frac{Q}{i \cdot t - 0 \cdot 1Q} i^* - K \frac{Q}{Q - i \cdot t} i \cdot t + Ae^{-B \cdot i \cdot t} \tag{1}$$

In discharging mode, the equation of the voltage source of lithium-ion battery is described as [44]:

$$V_{batt} = U_0 - R \cdot i - K \frac{Q}{Q - i \cdot t} i^* - K \frac{Q}{Q - i \cdot t} i \cdot t + Ae^{-B \cdot i \cdot t} \tag{2}$$

The state of charge (SOC) equation is based on coulomb counting method. This method is simple to implement but the initial SOC value should be known. The equation is written as follows [45]:

$$SOC = 100 \left(1 - \frac{i \cdot t}{Q} \right) \tag{3}$$

In order to accomplish the demand of total voltage and current levels, many Li-ion battery cells are connected in series and/or parallel configurations. The association of battery cell in series and parallel determines a battery pack.

The series number cell of a battery pack N_S is calculated as [46]:

$$N_S = \frac{U_{DC}}{U_0} \tag{4}$$

The number of parallel cells of battery packs N_P is expressed as [46]:

$$N_P = \frac{E_{bat}}{(E_{cell} - \Delta_{E-w} \cdot w_{cell}) \cdot N_S} \tag{5}$$

With:

$$\Delta_{\mathrm{E-w}} = \alpha \cdot 1,4 \tag{6}$$

The parameters of the studied PEVs battery cell are detailed in the Appendix.

The SOC of the studied batteries should be maintained in an operating range of limits in order to avoid the over-charge and the deep discharge of the battery:

$$SOC_{min} \le SOC \le SOC_{max} \tag{7}$$

With:$SOC_{min} = 0,2, \quad SOC_{max} = 0,8.$

The SOC depends on the distance run by each PEV. The demanded energy for traveling P_{tr} depends on the distance run AD and the vehicle efficiency μ_{PEV} as given in Ref. [47]:

$$P_{tr} = \mu_{PEV} \cdot AD \tag{8}$$

3. Control of PEV power generation

The control of each PEV power generation is achieved by the control of the different power converters. This control, summarized in Fig. 2, is classified into three parts. The first one illustrates the control the DC/DC converter and the battery current.

-Current control: A PI regulator is used to adapt the battery charge or discharge current to the reference value"$I_{bat-ref}$". While the positive battery current corresponds to a discharge phase, the

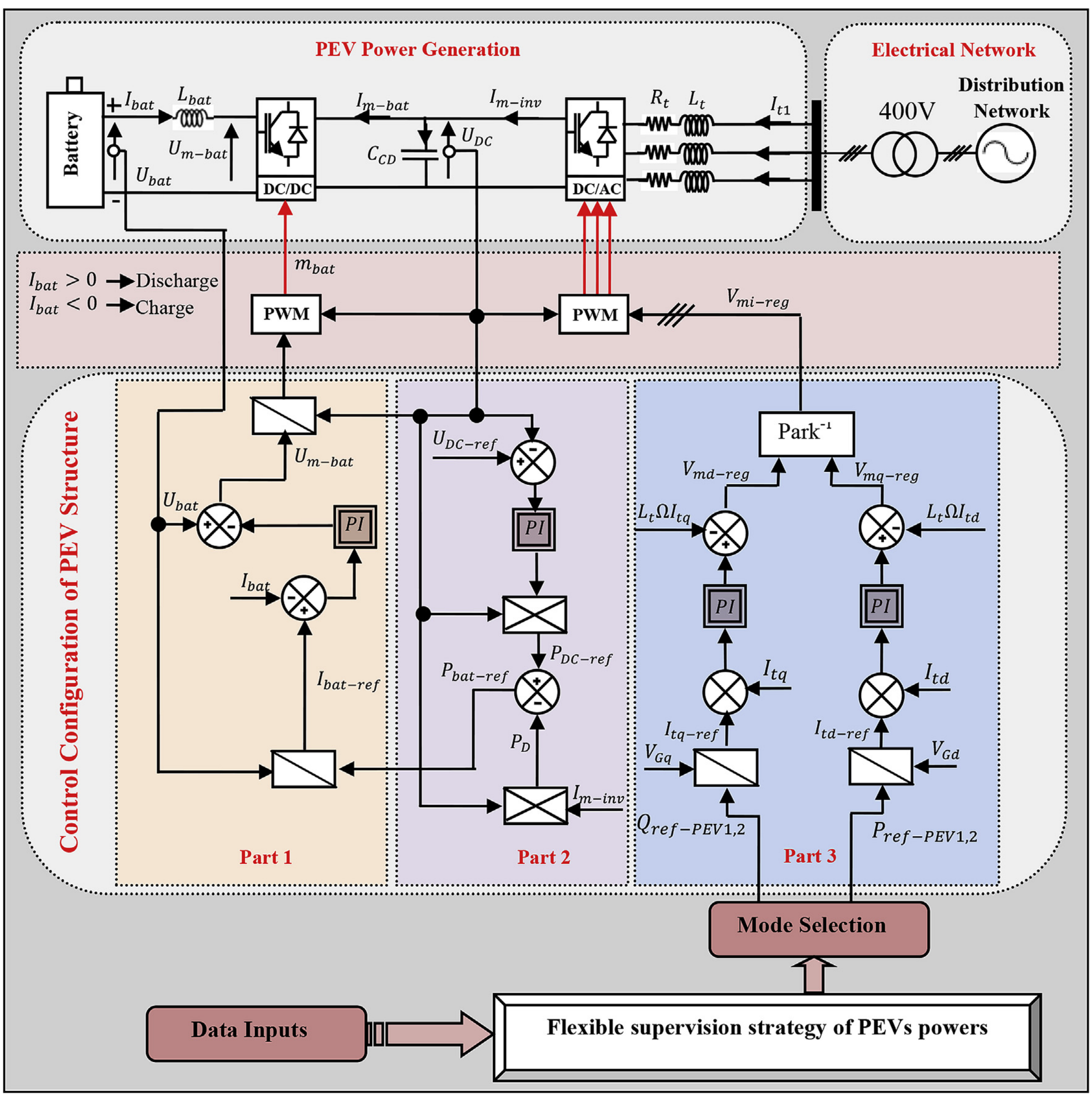

Fig. 2. Control configuration of each PEV structure for power generation.

negative battery current corresponds to a charge phase. This PI regulator is expressed by the following equation:

$$U_{m-bat} = U_{bat} - PI\left(I_{bat-ref} - I_{bat}\right) \tag{9}$$

-Converter control: The main role of DC/DC converter is to adapt the battery output voltage to the adequate inverter input voltage. The control of the DC/DC converter is given by the duty ratio as follow:

$$m_{bat-ref} = \frac{U_{m-bat}}{U_{DC}} \tag{10}$$

The second part corresponds to the DC bus control. A PI regulator is used to control the DC bus voltage by setting the reference current$''I_{bat-ref}''$. Then, the reference of the battery exchanged power $''P_{bat-ref}''$ can be calculated taking into account the needed power to control the DC bus voltage$''P_{DC-ref}''$ and the power to satisfy demands$''P_D''$, as given by the following equation.

$$P_{bat-ref} = P_{DC-ref} - P_D \tag{11}$$

Indeed, the DC bus control depends mainly on the proposed strategy which consists in controlling the battery state and calculating its needed reference power to be absorbed or supplied.

The third part which is depicted in Fig. 2 presents the DC/AC converter control and currents control Indeed, the bidirectional DC/AC converter ensures the control of the continuous voltage in grid side as well as the exchange of active and reactive powers between the PEVs and the grid. The injected or the absorbed currents are regulated according to the different operating modes of the proposed algorithm. This algorithm is developed to monitor the power flows between each PEV and the power grid in order to make decision to choose correctly the optimal references PEV powers $P_{PEV1,2-ref}$ and to ensure a flatter daily load power curve.The reactive power Q_{ref} is set to zero to ensure a power factor equals to one. These reference powers yield the components park reference currents$''i_{td-ref}, i_{tq-ref}''$ for active and reactive powers management goal. From the continuous voltage measurement and the modulated voltages, the operating of this converter is assisted by the computation of the reference phase voltages $''V_{md-reg}, V_{mq-reg}''$ according the following equations:

$$V_{md-reg} = \frac{2}{U_{DC}} V_{md} \tag{12}$$

$$V_{mq-reg} = \frac{2}{U_{DC}} V_{mq} \tag{13}$$

These voltages are used to generate the duty cycles of the inverter control signals. In order to regulate the line-to-line voltages, attenuate the generated harmonics and realize good performances in tracking, two PI correctors are used to control the connection line. This control permits, simultaneously the three-phase voltage at the nominal frequency 50 Hz. The active and reactive powers transmitted into the grid through the line are calculated as follows:

$$P_{Grid} = V_{Gd}\, i_{td} + V_{Gq}\, i_{tq} \tag{14}$$

$$Q_{Grid} = V_{Gq}\, i_{td} - V_{Gd}\, i_{tq} \tag{15}$$

4. Proposed control strategy

In order to achieve an optimal flow of PEVs powers in smart grid transaction, a power control strategy is investigated. The considered approach is applied for any house equipped with two PEVs. This strategy, depicted in Fig. 3, permits power dispatching between these two PEVs and power grid and aims to minimize the load power variance. Seven operating modes are considered to calculate the optimal reference powers of the two PEVs $''P_{ref-PEV1,2}''$ absorbed or injected to the grid in case of lack or excess in load demand, respectively. The proposed algorithm which is built on “flexible supervision strategy of PEVs powers” as well as monitoring the system correctly into seven operating modes is established to ensure the following roles:

- Receiving the daily load configuration data that describe the studied household appliances, the connection state of the two PEVs and the SOC of each battery.
- Establishing the priority order between these two PEVs with certain flexibility.
- Assuring the power management between the PEVs and loads in order to reduce the stress of the electrical grid and achieve the smoothness for the power demand curve.
- Controlling the batteries SOC and consequently avoiding the deep discharge and overcharge of the batteries.

There are several conditions which are essential to ensure the functioning of the algorithm suggested above. First, the proper connection status of each PEV in which a specific PEV plugs-in at the first of sometime-period and plugs-out at another time-period must be ensured. Second, it is essential to maintain the initial value of SOC of each considered PEV battery. Indeed, equation (7) demonstrates the allowed minimum and maximum battery SOC of the studied PEVs which need to be sustained within the allowable levels to save the battery from deterioration and reduce battery degradation. Finally, the total load power$''P_L''$ presented by daily load profile and the reference average power of the studied home$''P_R''$ are to be well maintained. It is assumed that the average reference power consists on the average household load power and the average required power for the distance run by each PEV as expressed in equation (16).

$$P_R = \frac{1}{T}\sum_{t=1}^{T}(P_L + P_{PEV1} + P_{PEV2}) \tag{16}$$

The control is done by calculating the amount of PEVs powers needed to be absorbed or injected into the power grid $''P_{diff}''$ by the considered equation:

$$P_{diff} = P_L - P_R \tag{17}$$

At each instant, the number, the connection time, the priority order of the considered PEVs and the sign of $''P_{diff}''$ are identified at the same time.

- When there is an excess of load demand "$P_{diff} \geq 0''$. In this situation,$''P_{diff}''$ should be injected into the grid from the PEVs. Moreover, if the battery SOC value of the PEV is equal or less than the SOC_{min}: the PEV must be connected and waits for charging. Else, if the battery SOC value is more than the SOC_{min}, then it is the V2G operation case. Indeed, the PEV acts to decrease the excess required energy and feedback the stored power into the grid.
- When there is a lack of power consummation$''P_{diff} < 0''$. In this situation, $''P_{diff}''$ should be absorbed from the grid. If the battery

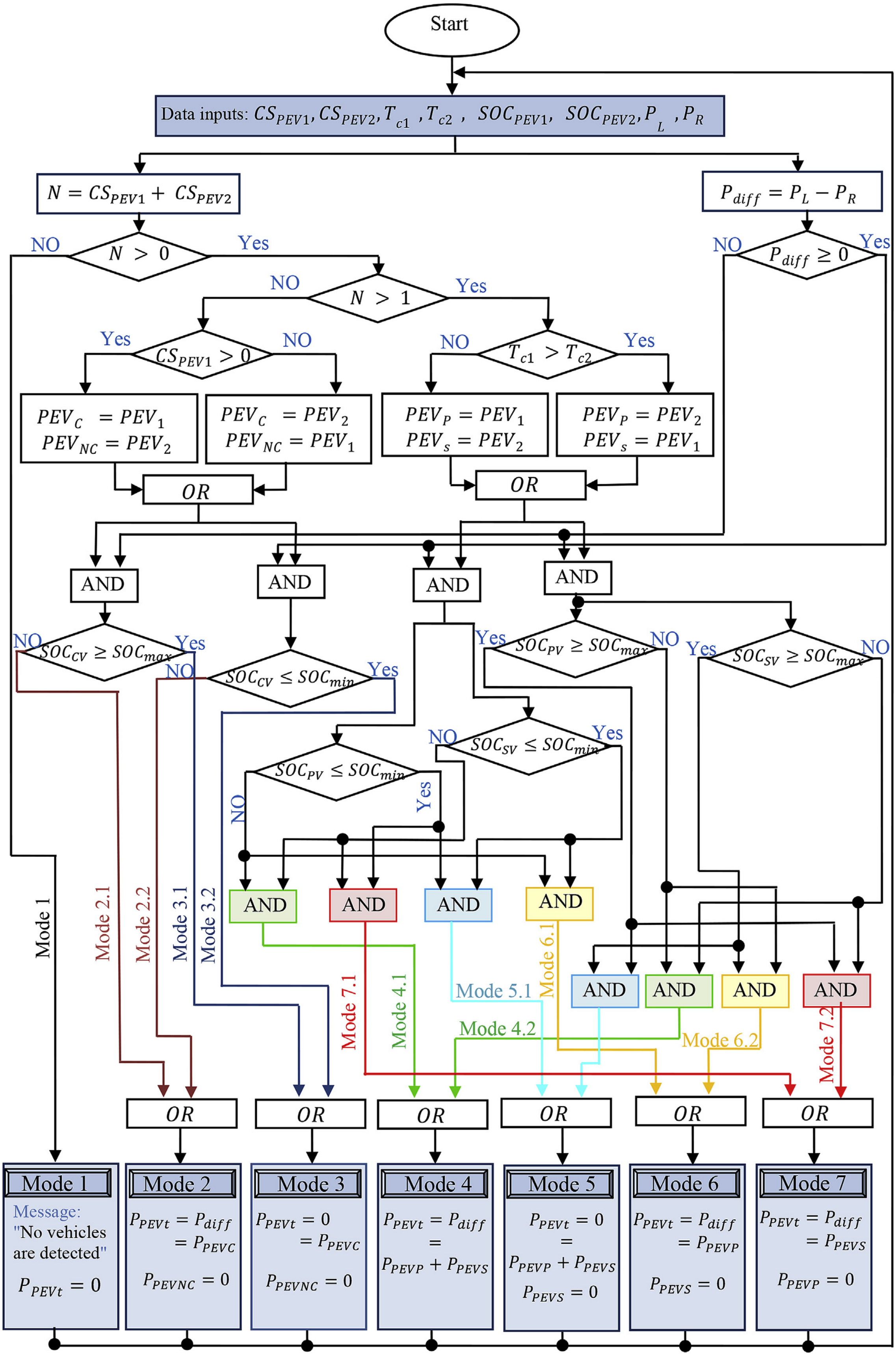

Fig. 3. Flexible supervision strategy of PEVs powers.

SOC value of the PEV is equal or more than the SOC_{max}: the PEV is charged and it is ready for being used. Else, if the battery SOC value is less than the SOC_{max}, then it is the G2V operation. In fact, the PEV operates to compensate this lack and absorb the electric power from the grid.

This algorithm receives, first, the total load power $''P_L''$, the reference average power $''P_R''$, the connection status of PEV number one $''CS_{PEV1}''$, the connection status of PEV number two $''CS_{PEV2}''$, the connection time of PEV number one $''T_{c1}''$, the connection time of PEV number two $''T_{c2}''$, the battery SOC value of PEV number one $''SOC_{PEV1}''$ and the battery SOC value of PEV number two $''SOC_{PEV2}''$, as inputs, then, it is managed into seven operating modes:

4.1. Mode 1

This mode shows that no PEVs are connected to the grid. In this case: the number of PEVs is equal to zero and the total PEVs power is also equal to zero $''P_{PEVt} = 0''$ because there is no power transmitted to the grid.

4.2. Mode 2

This is the mode where one PEV is at home and is available to join V2G or G2V operation. In this mode: the number of PEVs detected is $''N = 1''$ which means that the connection status of PEV number one is equal to one or connection status of PEV number two is equal to one. $''CS_{PEV1} = 1 \quad or \quad CS_{PEV2} = 1''$.

The first case of mode 2 (mode 2.1) is obtained when $''P_{diff}''$ is negative and the SOC of the connected vehicle $''SOC_{cv}''$ is less than the SOC_{max}, thus the PEV operates to compensate the lack of energy and absorb this quantity of power from the grid.

The second case of mode 2 (mode 2.2) is detected when $''P_{diff}''$ is positive and the SOC of the connected vehicle $''SOC_{cv}''$ is more than the SOC_{min}, so there is an excess of demand and the power quantity needed $''P_{diff}''$ should be injected to the grid through this PEV.

According to these two cases: the power of PEV, when it is not connected, is equal to zero $''P_{PEVNC} = 0''$ and the total PEVs power is equal to $''P_{diff}''$ which is equal also to the power of connected vehicle $''P_{PEVt} = P_{PEVC}''$.

4.3. Mode 3

It corresponds also to the availability of one PEV $''N = 1''$ and $''CS_{PEV1} = 1 \quad or \quad CS_{PEV2} = 1''$, but the connected vehicle expects the minimum or the maximum SOC. This mode is obtained by two cases:

If $''P_{diff}''$ is negative and $''SOC_{cv}''$ is equal or more than the SOC_{max}, thus the PEV is totally charged and ready for being used. It is in the first case of mode 3 (mode 3.1) where the battery attends its maximum $''SOC_{cv} = SOC_{max}''$.

If $''P_{diff}''$ is positive and $''SOC_{cv}''$ is equal or less than the SOC_{min}, thus the connected PEV must wait for charging because its battery expects its $''SOC_{min}''$. It is the second case of mode 3 (mode 3.2).

The two cases stated above indicate that the $''P_{PEVNC} = 0''$ and the total PEVs power is equal to the power of connected vehicle which is equal to zero $''P_{PEVt} = P_{PEVC}''$.

The following modes 4, 5, 6 and 7 will appear when there are two PEVs $''N = 2''$, $''CS_{PEV1} = 1 \; and \; CS_{PEV2} = 1''$. In this situation, we have:

4.4. Mode 4

This mode is obtained by the activation of one of these two cases:

When $''P_{diff}''$ is positive, the SOC of priority vehicle $''SOC_{pv}''$ is more than the SOC_{min} and the SOC of secondary vehicle $''SOC_{sv}''$ is more than the SOC_{min}, this is the first case of mode 4 (mode 4.1) which is responsible for the discharging of the priority and the secondary PEVs and feed backing power to the grid.

When $''P_{diff}''$ is negative, the $''SOC_{pv}''$ is less than the SOC_{max} and the $''SOC_{sv}''$ is less than the SOC_{max}, which is the second case of this mode (mode 4.2). This case is responsible for charging the priority and the secondary PEVs.

Considering the two cases mentioned above, the total PEVs power is calculated from the power of the priority PEV and the power of the secondary PEV which is equal to: $''P_{PEVt} = P_{PEVP} + P_{PEVS}''$.

4.5. Mode 5

There are, in this mode, two selected cases:

If $''P_{diff}''$ is positive, the $''SOC_{pv}''$ is equal or less than the SOC_{min} and the $''SOC_{sv}''$ is equal or less than the SOC_{min}, the first case of mode 5 (mode 5.1) is obtained. It is the case in which the batteries of priority and secondary PEV reach their minimum SOC value. Hence, these two PEVs should be connected and wait for charging.

If $''P_{diff}''$ is negative, the $''SOC_{pv}''$ is equal or more than the SOC_{max} and the $''SOC_{sv}''$ is equal or more than the SOC_{max}, the second case of mode 5 (mode 5.2) shows that the priority and secondary PEVs are completely charged and ready for being used because the batteries SOC value attain their maximum value $''SOC_{max}''$.

These two cases demonstrate that there is no power exchanged with the grid. Indeed, the power of the priority PEV is equal to zero $''P_{PEVP} = 0''$, the power of the secondary PEV is equal to zero $''P_{PEVS} = 0''$ and the total PEVs power is equal to: $''P_{PEVt} = P_{PEVP} + P_{PEVS}''$.

4.6. Mode 6

In this mode, there are two interactive cases to distinguish:

When $''P_{diff}''$ is positive, the $''SOC_{pv}''$ is more than the SOC_{min} and the $''SOC_{sv}''$ is equal or less than the SOC_{min}, which is the first case of this mode (mode 6.1). The priority PEV is in discharging phase which can inject the stored power to the grid and consequently minimize load power variance, whereas, the secondary PEV attends its $''SOC_{min}''$ and must wait for charging.

When $''P_{diff}''$ is negative, the $''SOC_{pv}''$ is less than the SOC_{max} and the $''SOC_{sv}''$ is equal or more than the SOC_{max}, which is the second case of this mode (mode 6.2). The priority PEV is in charging phase

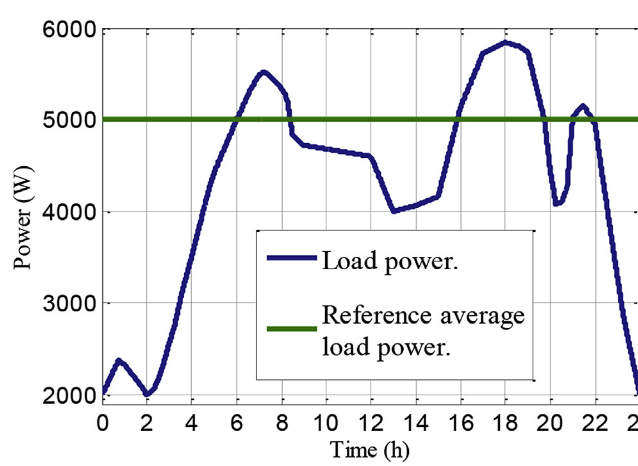

Fig. 4. Total load power without PEV connection.

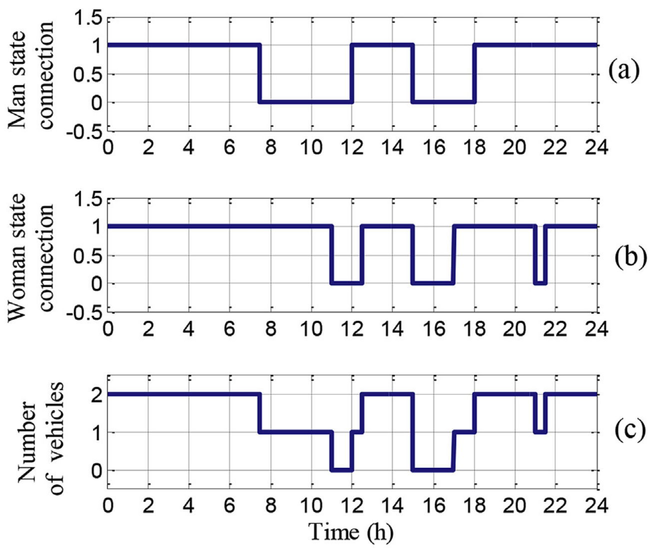

Fig. 5. Connection status of each PEV: (a) Man state connection. (b) Woman state connection. (c) Number of vehicles.

and the secondary PEV is ready for being used because it attains its $''SOC_{max}''$.

These two cases of this mode prove that: $''P_{PEVS} = 0''$ and $''P_{PEVt} = P_{PEVP}''$.

4.7. Mode 7

This mode is active when one of these two cases is obtained:

If $''P_{diff}''$ is positive, the $''SOC_{pv}''$ is equal or less than the SOC_{min} and the $''SOC_{sv}''$ is more than the SOC_{min}, which the first case of this mode (mode 7.1) is active, the studied algorithm calculates the required power that should be injected to the grid by the secondary PEV. In addition, the priority PEV reaches its $''SOC_{min}''$ and must wait for charging.

If $''P_{diff}''$ is negative, the $''SOC_{pv}''$ is equal or more than the SOC_{max} and the $''SOC_{sv}''$ is less than the SOC_{max}, which the second case of mode 7 (mode 7.2) is active, the studied algorithm calculates the required power that should be absorbed from the grid by the secondary PEV. Furthermore, the priority PEV is fully charged and it is ready for being used $''SOC_{pv} = SOC_{max}''$.

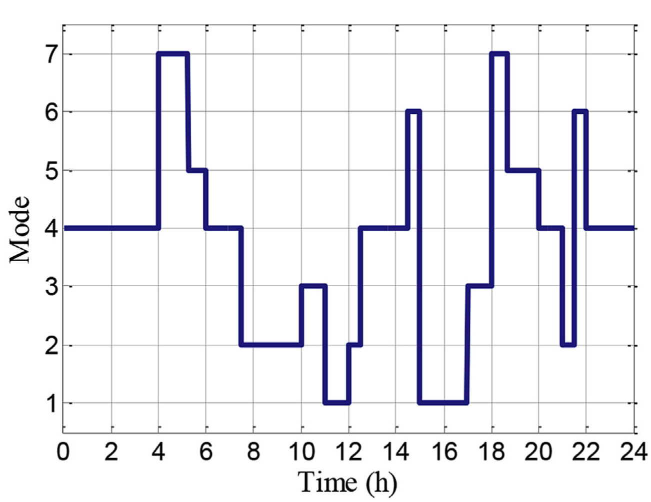

Fig. 6. Different operating modes.

This mode ensue the following results: $''P_{PEVP} = 0''$ and $''P_{PEVt} = P_{PEVS}''$.

5. Simulation results

In order to validate the effectiveness of the proposed control strategy, simulation of the daily load demand curve smoothness was implemented. The obtained results were investigated to verify the different operating modes.

This approach was evaluated taking into account of the power demand except for the PEVs connection which is depicted in Fig. 4, the PEVs number, the connection status of each PEV and their initial SOC. In this study, it is assumed that the maximum number PEVs is two, one for a man and anther for a woman, where charging/discharging phenomena are taking place in a residential location (at home). The domestic load profile is based on the actual consumption patterns of a family who lives within a necessary life. The average power load is calculated taking into account the average daily load consumption and the average daily PEVs consumption.

The batteries capacities of the man PEV and the woman PEV are 14 kWh and 11 kWh. Respectively the minimum and maximum SOC limitations are set as 0.2 and 0.8. The power of each PEV boundaries is selected: the minimum operating power to be supplied to the PEV is $P_{PEV-min} = -1.5\,KW$ and the maximum operating PEV power to be injected to the grid is$P_{PEV-max} = 1.5\,KW$.

To facilitate calculation, the simulations are done during one day which is split into T time-periods where the length of each time-period Δt is fixed at 15 min. Thus, there are 96 intervals during the day. The priority order is chosen as the first PEV coming and plugging into the house parking. Indeed, any time chosen may be involved to join V2G operation by fixing the adequate time-period which ensures the flexibility of the operation. Consequently, these PEVs are assumed to begin charging at the start of a given time-period and stops charging at the end of another time-period.

As shown in Fig. 5, the man PEV is plugged-in at 18 h and plugged-out at 7:30 h of the next day. During [7:30, 12 h], this PEV is unavailable to join smart grid system. At 12 h, he comes back home for lunch and leaves at 15 h. During [15, 18 h], the man PEV is not at home.

In this scenario chosen, the woman PEV leaves home at 11 h and returns at 12:30 h. Then, she leaves at 15 h in the afternoon and rejoins the V2G operation at 17 h in the evening. During [21, 21:30 h], the PEV woman leaves home parking.

The PEVs number is deducted from the sum of connection status of man and woman PEVs.

$$''N = CS_{PEV1} + CS_{PEV2}'' \tag{18}$$

The algorithm operating is well explicated in section 4, and according it the PEV's seven operating modes of the total power are recognized. Fig. 6 and Fig. 7 show the seven operating modes and the different cases of the deduced modes form this strategy, respectively.

During the following periods [0, 4 h], [12:30, 14:30 h], [20, 21 h] and [22, 24 h], the proposed algorithm operates in mode 4.2 which is the charging of the man and woman PEVs. However, the discharge of both PEVs in mode 4.1 is done during [6, 7:30 h]. During these periods in where mode 4 is active, the total power given by the sum of the priority PEV power and secondary PEV power can considerably flatten the daily load power curve.

In the intervals [4, 5:15 h] and [18, 18:40 h], mode 7 is active where the first interval corresponds to case of mode 7.2 and the second interval corresponds to case of mode 7.1. The total power is calculated only from the secondary PEV power because the priority PEV battery expects the $''SOC_{min}''$ or the $''SOC_{max}''$.

In the periods [5:15, 6 h] and [18:40, 20 h], the mode 5.2, where

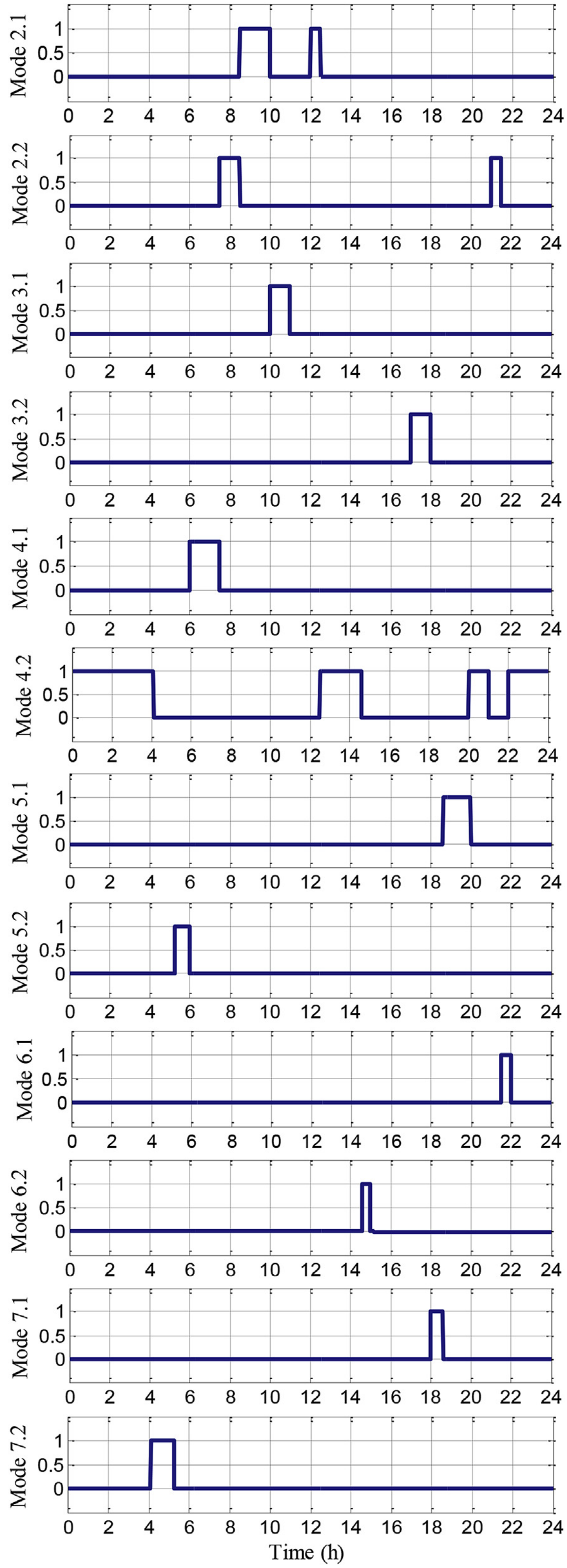

Fig. 7. Different interactive cases of the deduced modes.

priority and secondary PEVs are totally charged and reached the "SOC_{max}", and mode 5.1, where priority and secondary PEVs reach the "SOC_{min}", are respectively detected. During these periods, mode 5 is observed in which no PEVs powers are exchanged and,

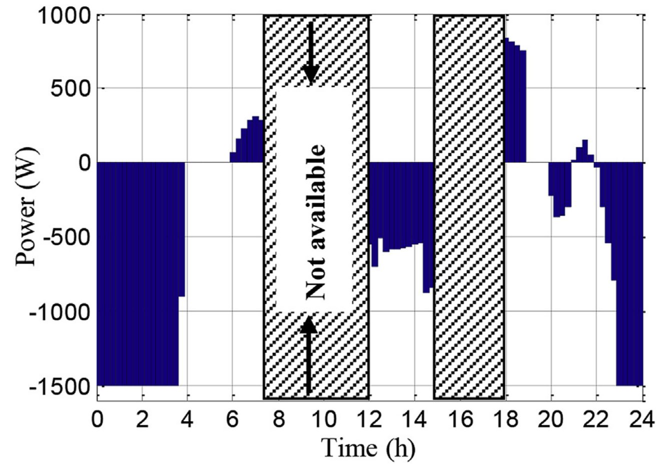

Fig. 8. Charging profile of man PEV.

consequently, the total PEVs power calculated from the sum of the priority PEV power and secondary PEV power is equal to zero.

In the intervals [7:30, 10 h], [12, 12:30 h] and [21, 21:30 h], mode 2 is obtained where the total power is calculated from only the PEV connected to home parking. Indeed, during [7:30, 8:30 h] and [21, 21:30 h], mode 2.2 is active. The first period corresponds to woman PEV injection power; however, the second period corresponds to man PEV injection power. During [8:30, 10 h] and [12, 12:30 h], mode 2.1 is obtained. In the first interval, woman PEV absorbs power from the grid. Whereas, man PEV absorbs power from the grid in the second interval.

In the periods [10, 11 h] and [17, 18 h], the total power determined by the woman PEV power is equal to zero because the battery attained its "SOC_{max}" in the first interval corresponding to mode 3.1 and it reaches its "SOC_{min}" in the second interval corresponding to mode 3.2. During these two periods, mode 3 is active.

In the time [11, 12 h], mode 1 is observed in which no PEVs are detected and, consequently, the total PEVs power is equal to zero which is the same result in the following interval [15, 17 h].

During [14:30, 15 h] and [21:30, 22 h], mode 6 is functional in which the total power is given only by the priority PEV power (man PEV). In fact, the woman PEV (secondary PEV) expects its "SOC_{max}" in the period [14:30, 15 h] corresponding to case 2 of mode 6. Whereas, it reaches its "SOC_{min}" during [21:30, 22 h] corresponding to case 1 of mode 6.

Fig. 8 and Fig. 9 illustrate the charging profiles of man PEV and

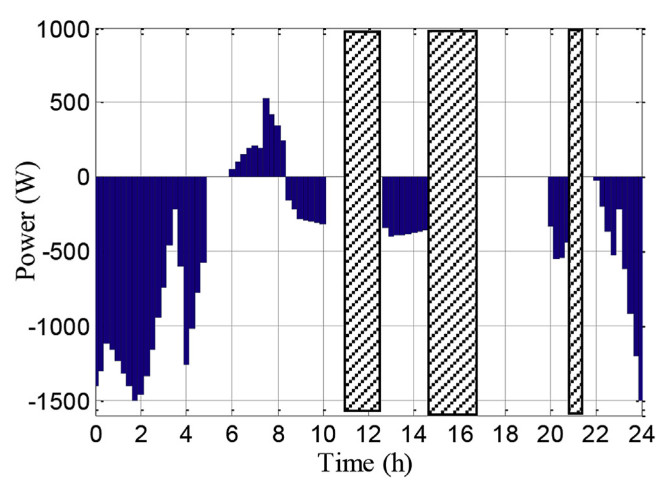

Fig. 9. Charging profile of woman PEV.

woman PEV during one day cycle. They show that the negative powers correspond to charging cases where both PEVs consume the difference power between the daily power requirement and the reference average power"P_{diff}". Whereas, the positive powers correspond to discharging cases where PEVs feedback the stored power to the grid.

From the power profile of man PEV, it is observable that, during [7.30, 12 h] and [15, 18 h], the man PEV does not absorb or supply electrical power because it is not connected from the grid. As far as, in the following intervals [11, 12 h], [15, 17 h] and [21, 21:30 h], the woman PEV is not at home and, consequently it does not join the V2G system.

Both man and woman battery current curves are shown in Fig. 10 and Fig. 11, respectively. These results confirm the chosen convention in which negative currents are dedicated for charging cases and positive currents for discharging cases.

The charging/discharging operation can be also confirmed by the evolution of battery SOC curve in time as presented in Fig. 12 and Fig. 13. As it seen, both man PEV and woman PEV have a specific SOC curve for their batteries during one day. It is notable that the PEV charging and discharging will be established according to initial SOC value in every connection to the grid. It is observable also that the discharging is accompanied with a little diminution of SOC curves of both batteries.

Fig. 14 shows the comparison of the power curves. It can be deducted that, by the implementing of this control algorithm, the daily load demand curve can be considerably flatten. Indeed, the total load power curve with PEVs connection in red coincides with the reference average power load curve in green during charging or

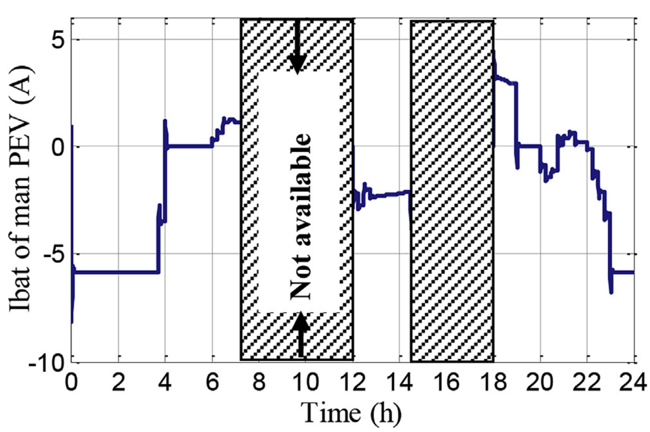

Fig. 10. Man battery current curve.

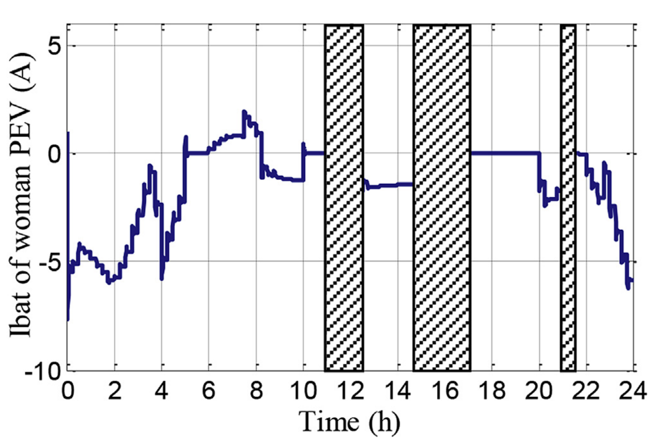

Fig. 11. Woman Battery current curve.

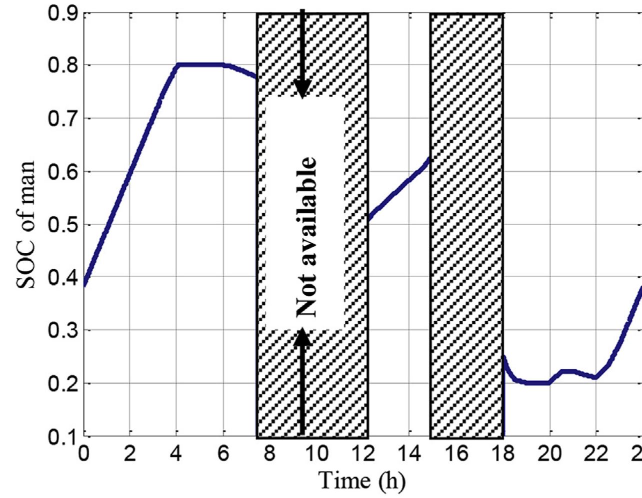

Fig. 12. State of charge curve of man PEV.

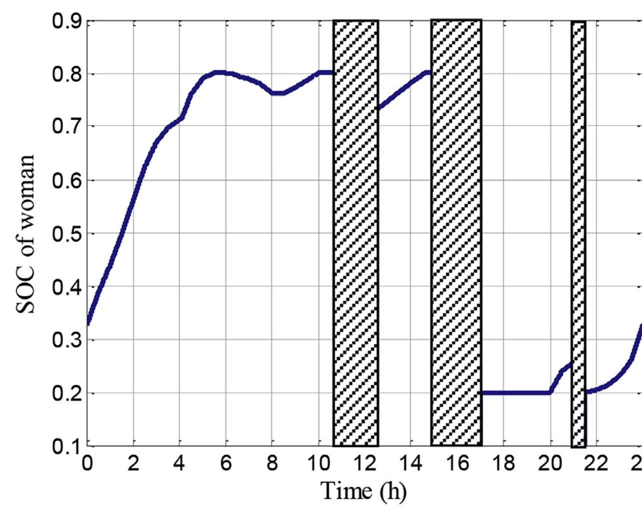

Fig. 13. State of charge curve of woman PEV.

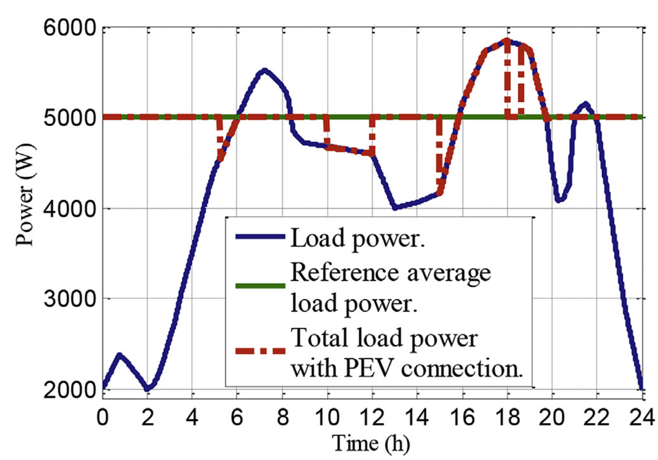

Fig. 14. Comparison of load power curves.

discharging operation. Whereas, the total power load in blue curve remains unchanged which is in the case where PEVs are not connected or not available to supply the stored energy to the grid.

6. Conclusion

In this paper, a flexible control strategy of two PEVs operating in seven modes is investigated. This control allows the detection of PEVs with their priority order in a first step and the availability of these PEVs to switch between different operating modes of activation with certain flexibility in a second step. The aim of this proposed algorithm was to manage the bi-directional power flow between the considered PEVs and power grid in order to achieve a smooth daily load power curve. This technique favors the integration of regulated charging of PEVs connected to home parking in order to provide grid support by injection or absorption of their optimal required powers and avoid the high electricity demand especially in peak hours. Simulation results were implemented to prove the effectiveness of the applied approach, its ability to flatten the total power demand curve and therefore to enhance the AC grid power qualities. This strategy can be generalized at each node and therefore for the whole network.

Appendix

Li-ion battery cell (3.3V, 2.3 A h) parameters.

Parameters	Value
Battery constant voltage	3.366 V
Internal resistance	0.01 Ω
Constant Polarization	0.0076 Ω
Exponentiel zone amplitude	0.26422 V
Exponential zone inverse constant time	26.5487 $(Ah)^{-1}$
Weight of the battery cell	0.07 Kg
Slope of PEV inclination	0.025
Battery cell energy	7.59Wh

References

[1] Andrews J, Shabani B. Dimensionless analysis of the global techno-economic feasibility of solar-hydrogen systems for constant year-round power supply. Int J Hydrogen Energy 2012;37:6–18.
[2] Askarzadeh A. A discrete chaotic harmony search-based simulated annealing algorithm for optimum design of PV/wind hybrid system. Sol Energy 2013;97:93–101.
[3] Belfkira R, Zhang L, Barakat G. Optimal sizing study of hybrid wind/PV/diesel power generation unit. Sol Energy 2011;85:100–10.
[4] Doucette R, McCulloch M. Modeling the prospects of plug-in hybrid electric vehicles to reduce CO2 emissions. Appl Energy 2011;88:2315–23.
[5] Arslan O, Karasan O. Cost and emission impacts of virtual power plant formation in plug-in hybrid electric vehicle penetrated networks. Energy 2013;60:116–24.
[6] Niknam T, Zare M, Aghaei J. Scenario-based multi-objective volt/var control in distribution networks including renewable energy sources. IEEE Trans Power Deliv 2012;27:2004–19.
[7] Boukettaya G, Krichen L. A dynamic power management strategy of a grid connected hybrid generation system using wind, photovoltaic and flywheel energy storage system in residential applications. Energy 2014;71:148–59.
[8] García –Villalobos J, Zamora I, San Martín JI, Asensio FJ, Aperribay V. Plug-in electric vehicles in electric distribution networks: a review of smart charging approaches. Renew Sustain Energy Rev 2014;38:717–31.
[9] Poullikkas A. Sustainable options for electric vehicle technologies. Renew Sustain Energy Rev 2015;41:1277–87.
[10] Zhao Z, Lee W, Shin Y, Song K. An optimal power scheduling method for demand response in home energy management system. IEEE Transanctions Smart Grid 2013;4. 139–400.
[11] Lund H, Mathiesen BV. Energy system analysis of 100% renewable energy systems - the case of Denmark in years 2030 and 2050. Energy 2009;34:524–31.
[12] Mathiesen BV, Lund H, Connolly D, Wenze H, Østergaard PA, Möller B, et al. Smart Energy Systems for coherent 100% renewable energy and transport solutions. Appl Energy 2015;145:139–54.
[13] Thakur J, Chakraborty B. Intelli-grid: moving towards automation of electric grid in India. Renew Sustain Energy Rev 2015;42:16–25.
[14] Siano P. Demand response and smart grids -A survey. Renew Sustain Energy Rev 2014;30:461–78.
[15] Deng R, Yang Z, Chen J, Asr N, Chow M. Residential energy consumption scheduling: a coupled-constraint game approach. IEEE Trans Smart Grid 2014;5:1340–50.
[16] Brouwer A, Kuramochi T, Broek M, Faaij A. Fulfilling the electricity demand of electric vehicles in the long term future: an evaluation of centralized and decentralized power supply systems. Appl Energy 2013;107:33–51.
[17] Su W, Chow M. Computational intelligence-based energy management for a large-scale PHEV/PEV enabled municipal parking deck. Appl Energy 2012;96:171–82.
[18] Honarmand M, Zakariazadeh A, Jadid S. Optimal scheduling of electric vehicles in an intelligent parking lot considering vehicle-to-grid concept and battery condition. Energy 2014;65:572–9.
[19] Amirioun MH, Kazemi A. A new model based on optimal scheduling of combined energy exchange modes for aggregation of electric vehicles in a residential complex. Energy 2014;69:186–98.
[20] Zhang J, He L, Li C, Cao Y, Wang J, Fang B, et al. Coordinated control for large-scale EV charging facilities and energy storage devices participating in frequency regulation. Appl Energy 2014;123:253–62.
[21] Sortomme E, Hindi M, Macpherson S, Venkata S. Coordinated charging of plug-in hybrid electric vehicles to minimize distribution system losses. IEEE Trans Smart Grid 2011;2:189–205.
[22] Foley A, Tyther B, Calnan P, Gallachoir B. Impacts of electric vehicle charging under electricity market operations. Appl Energy 2013;101:93–102.
[23] Drude L, Junior L, Rüther R. Photovoltaics (PV) and electric vehicle-to-grid (V2G) strategies for peak demand reduction in urban regions in Brazil in a smart grid environment. Renew Energy 2014;68:443–51.
[24] Lund H, Kempton W. Integration of renewable energy into the transport and electricity sectors through V2G. Energy Policy 2008;36:3578–87.
[25] Lund H. Renewable energy strategies for sustainable development. Energy 2007;32:912–9.
[26] Shafie-khah M, Neyestani N, Damavandi M, Gil F, Catalão J. Economic and technical aspects of plug-in electric vehicles in electricity markets. Renew Sustain Energy Rev 2016;53:1168–77.
[27] He Y, Venkatesh B, Guan L. Optimal scheduling for charging and discharging of electric vehicles. IEEE Trans Smart Grid 2012;3:1095–105.
[28] Gerssen-Gondelach S, Faaij A. Performance of batteries for electric vehicles on short and longer term. J Power Sources 2012;212:111–29.
[29] Hu X, Li SE, Jia Z, Egardt B. Enhanced sample entropy-based health management of Li-ion battery for electrified vehicles. Energy 2014;64:953–60.
[30] Yang S, Yao J, Kang T, Zhu X. Dynamic operation model of the battery swapping station for EV (electric vehicle) in electricity market. Energy 2014;65:544–9.
[31] Vardakas JS, Zorba N, Verikoukis CV. Scheduling policies for two-state smart home appliances in dynamic electricity pricing environments. Energy 2014;69:455–69.
[32] Gils HC. Assessment of the theoretical demand response potential in Europe. Energy 2014;67:1–18.
[33] Setlhaolo D, Xia X, Zhang J. Optimal scheduling of household appliances for demand response. Electr Power Syst Res 2014;116:24–8.
[34] Balta-Ozkan N, Davidson R, Bicket M, Whitmarsh L. The development of smart homes market in the UK. Energy 2013;60:361–72.
[35] Arghira N, Hawarah L, Ploix S, Jacomino M. Prediction of appliances energy use in smart homes. Energy 2012;48:128–34.
[36] Ha L, Ploix S, Zamai E, Jacomino M. Tabu search for the optimization of household energy consumption. In: IEEE international conference on information reuse and integration; 2006. p. 86–92.
[37] Faria P, Vale Z. Demand response in electrical energy supply: an optimal real time pricing approach. Energy 2011;36:5374–84.
[38] Jian L, Xue H, Xu G, Zhu X, Zhao D, Shao Z. Regulated charging of plug-in hybrid electric vehicles for minimizing load variance in household smart micro-grid. IEEE Trans Ind Electron 2013;60:3218–26.
[39] Lee Y, Khaligh A, Emadi A. Advanced integrated bidirectional AC/DC and DC/DC converter for plug-in hybrid electric vehicles. IEEE Trans Veh Technol 2009;58:3970–80.
[40] Keles C, Karabiber A, Akcin M, Kaygusuz A, Alagoz B, Gul O. A smart building power management concept: smart socket applications with DC distribution. Electr Power Energy Syst 2015;64:679–88.
[41] Sarasketa-Zabala E, Martinez-Laserna E, Berecibar M, Gandiaga I, Rodriguez-Martinez L, Villarreal I. Realistic lifetime prediction approach for Li-ion batteries. Appl Energy 2016;162:839–52.
[42] Jaguemont J, Boulon L, Dubé Y. A comprehensive review of lithium-ion batteries used in hybrid and electric vehicles at cold temperatures. Appl Energy 2016;164:99–114.
[43] Abada S, Marlair G, Lecocq A, Petit M, Sauvant-Moynot V, Huet F. Safety focused modeling of lithium-ion batteries: a review. J Power Sources 2016;306:178–92.
[44] Tremblay O, Dessaint L. Experimental validation of a battery dynamic model for EV applications. World Electr Veh 2009;3:289–98.
[45] Rahimi-Eichi H, Chow MY. Adaptive parameter identification and state-of

charge estimation of lithium-ion batteries. In: IEEE industrial electronics society conference in montreal, Canada; 2012. p. 4012–7.
[46] Sadoun R, Rizoug N, Bartholomeüs P, Barbedette B, Le Moigne P. Optimal sizing of hybrid supply for electric vehicle using Li-ion battery and supercapacitor. In: IEEE vehicle power and propulsion conference; 2011. p. 1–8.
[47] Soroudi A, Keane A. Risk averse energy hub management considering plug-in electric vehicles using information gap decision theory. In: Rajakaruna S, Shahnia F, Ghosh A, editors. Plug -in electric vehicles in smart Gri1ds: energy management. Springer: E-Publishing Inc; 2015. p. 107–27.

Nomenclature

U_{batt}: Battery voltage (V)
U_0: Battery constant voltage (V)
R: Battery internal resistance (Ω)
K: Constant Polarization (Ω)
i: Battery current (A)
$i.t$: Actual battery charge (Ah)
i^*: Battery filtered current (A)
Q: Battery capacity(Ah)
A: Exponentiel zone amplitude (V)
B: Exponential zone inverse constant time$(\mathrm{Ah})^{-1}$
Δ_{E-w}: Energy variation versus weight
α: Slope of PEV inclination
E_{cell}: Battery cell energy
w_{cell}: Weight of the battery cell
E_{bat}: Battery provided energy
N_S: Number of battery cells connected in series
N_P: Number of battery cells connected in parallel
μ_{PEV}: Efficiency of the vehicle
U_{m-bat}: Modulated voltage of DC/DC converter(V)
I_{m-bat}: Modulated current of the battery (A)
L_{bat}: Battery filter inductance (H)
U_{DC}, I_{DC}: DC bus voltage (V) and current (A)
C_{DC}: DC bus capacitance (μF)
i_{m-inv}: Inverter input current (A)
i_{td}, i_{tq}: d and q line currents (A)
$V_{md}, V_{mq},$: Direct and quadratic components of the DC/AC converter voltages (V)
V_{Gd}, V_{Gq}: Direct and quadratic components of Grid voltages (V)
Ω: rotational speed (rad s^{-1})
R_t: Line resistance (Ω)
L_t: Line inductance (H)
N: Number of PEVs
CS_{PEV1}: Connection status of PEV number one
CS_{PEV1}: Connection status of PEV number two
T_{c1}: Connection time of PEV number one
T_{c2}: Connection time of PEV number two
P_L: Total load power in a home appliances
P_R: Reference average power of home
PEV_C: Connected PEV
PEV_{NC}: Not connected PEV
SOC_{min}: Minimum value of the battery SOC
SOC_{max}: Maximum value of the battery SOC